

Periodic alignment of Si quantum dots on hafnium oxide coated single wall carbon nanotubes

Mario Olmedo,¹ Alfredo A. Martinez-Morales,¹ Gang Liu,² Emre Yengel,³ Cengiz S. Ozkan,³ Chun Ning Lau,² Mihrimah Ozkan,¹ and Jianlin Liu^{1,a)}

¹Department of Electrical Engineering, University of California, Riverside, California 92521, USA

²Department of Physics and Astronomy, University of California, Riverside, California 92521, USA

³Department of Mechanical Engineering, University of California, Riverside, California 92521, USA

(Received 22 December 2008; accepted 3 March 2009; published online 26 March 2009)

We demonstrate a bottom up approach for the aligned epitaxial growth of Si quantum dots (QDs) on one-dimensional (1D) hafnium oxide (HfO₂) ridges created by the growth of HfO₂ thin film on single wall carbon nanotubes. This growth process creates a high strain 1D ridge on the HfO₂ film, which favors the formation of Si seeds over the surrounding flat HfO₂ area. Periodic alignment of Si QDs on the 1D HfO₂ ridge was observed, which can be controlled by varying different growth conditions, such as growth temperature, growth time, and disilane flow rate. © 2009 American Institute of Physics. [DOI: 10.1063/1.3103547]

Si quantum dots (QDs) are utilized for a wide range of applications including traditional electronics such as memory,^{1,2} optoelectronics,^{3,4} and biotechnology.⁵ Single QD devices have been fabricated to outperform current devices such as field effect transistors⁶ for ultralarge scale integration. Several options are already available via top-down approaches such as electron beam lithography and nanostamping⁷ that can fabricate single QD devices. Another popular method is the growth of QDs via self-assembly instead of fabrication. One of the major hurdles in this approach is the alignment of the QDs themselves. Here we demonstrate a solution to Si QD alignment using a HfO₂ covered single wall carbon nanotube (SWCNT) template.

The template comprises of HfO₂ ridges formed by atomic layer deposition growth of a HfO₂ thin film on SWCNTs on a silicon dioxide (SiO₂) surface. The major advantage for the use of SWCNTs is in their one-dimensional (1D) shape and nanometer scale diameter, which will enable applications to go beyond the complementary metal-oxide-semiconductor (CMOS) ultimate limit. The technique of selective area epitaxy^{8,9} has reported the alignment of QDs on Si ridges. This technique starts with a top-down patterned template, followed by a bottom up growth of QDs. This process requires a smooth surface so that during the QD growth the adatoms can migrate to the lowest energy spots. Traditionally, single crystal surfaces have been used for the alignment of QDs via selective epitaxial growth or QD superlattice growth. The atomic layer deposition technique can produce HfO₂ thin dielectric films with smooth conformal polycrystalline surfaces, which can be used for QD self-assembly.¹⁰ QDs grown on HfO₂ surfaces may have potential applications in nonvolatile nanocrystal memories.

The experimental procedure is as follows. SWCNTs were grown on SiO₂/Si substrates using a chemical vapor deposition technique.^{11,12} The nanotube samples were then subjected to an UV cleaning for 5 min to make the substrate surface hydrophilic. This time was adjusted to ensure good precursor adhesion as well as keeping the CNTs intact. Fol-

lowing the surface treatment procedure, the samples were introduced to a Cambridge Nanotech Savannah 100 atomic layer deposition chamber. The system ran at a partial pressure of 3×10^{-1} torr and a deposition time of 5 s was used for both precursor and source. Substrate temperature for the HfO₂ deposition was kept constant at 250 °C. The Si QD deposition was done in a custom built gas source molecular beam epitaxy system. The disilane (Si₂H₆) source points directly at the substrate. The base pressure was in the order of 10⁻⁸ torr, while growth pressure was in the range of 10⁻⁵ torr. The samples were heated via a Ta heating coil that coupled with the sample holder. Temperature readings were taken by a thermocouple situated between the sample and the heating coil. The source gas flow was controlled using a mass flow controller UFC 1660. Atomic force microscopy (AFM) characterization was carried out using a Veeco multimode AFM.

Figure 1(a) shows a schematic of aligned Si QDs on HfO₂ covered CNTs formed by selective epitaxial growth. The QDs are drawn only on the 1D HfO₂ ridge created by the underlying CNTs. Other QDs could be formed on the surrounding flat surface depending on the magnitude of the length of Si adatom migration on HfO₂ and the proximity of adjacent CNTs. Figure 1(b) shows a cross-sectional SEM image of a QD alignment sample. The HfO₂ thickness is 6 nm and the ridge height was measured to be 1–1.2 nm by AFM characterization. QDs are clearly observed to align along the 1D HfO₂ ridge, while QDs are also seen on the flat surface close to the CNT ridge. The QDs on top of the CNT are larger in size demonstrating that more Si adatoms preferentially migrated to the 1D ridge. We hypothesized that if the density of CNTs is increased, selective growth of Si dots only on the ridges will be evident. The HfO₂ layer is highly conformal on the SiO₂ surface as the shape of the CNT is seen in the SEM image. The CNT surface however is not chemically active¹³ so fewer layers are deposited over the ridge than the rest of the film. This characteristic can be advantageous in a circuit setting by utilizing different thicknesses of the oxide film in between CNT channels¹⁴ as the local oxidation of silicon equivalent of isolating oxide.

^{a)}Author to whom correspondence should be addressed. Electronic mail: jianlin@ee.ucr.edu.

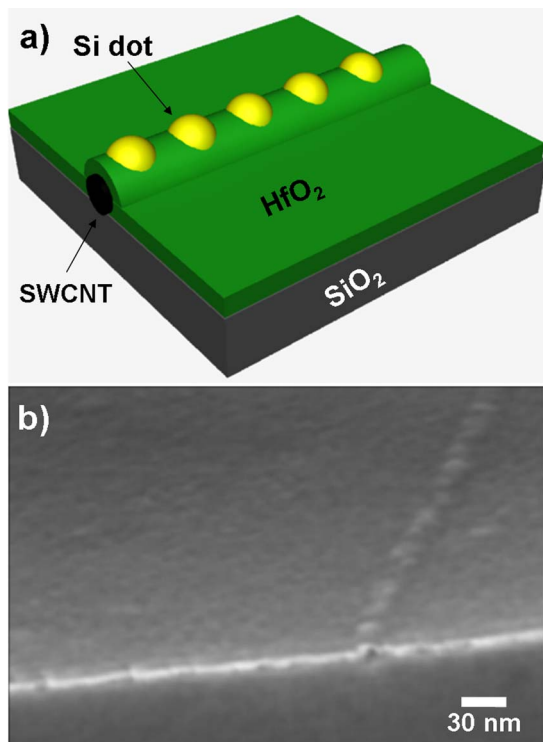


FIG. 1. (Color online) QDs on a hafnium oxide covered CNT. (a) Schematic of a cross-sectional view of the structure. (b) SEM image cross sectional shows aligned QDs on a HfO₂ covered CNT.

To ensure that the observed QDs on the surface are Si dots rather than HfO₂ grains due to annealing, an experiment comparing the annealed samples before and after disilane flow was introduced. Figures 2(a) and 2(b) show the AFM images of these samples. Both samples began with the 6 nm HfO₂ covered CNT. The *in situ* annealing including ramping from room temperature to 650 °C within 2 h and maintaining at this temperature for 8 min was used for both samples. The control sample which was not subjected to disilane growth shows relatively smooth surface, while the sample with disilane flow of 1.6 SCCM (SCCM denotes standard cubic centimeter per minute at STP) for 8 min shows rough surface with QD alignment.

The growth processes of the selective area epitaxy can be observed clearly through the changes in QD linear density. The QD linear density was obtained via AFM measurement along the CNT ridge. Figures 3(a)–3(d) show the morphology along the samples grown at different flow rates. A higher rate of disilane flow results in smaller and denser

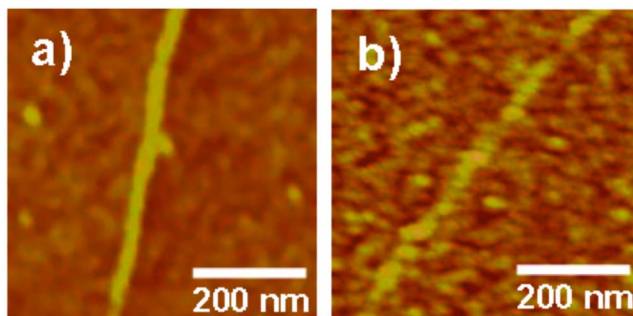


FIG. 2. (Color online) AFM images of HfO₂ covered CNT after *in situ* annealing, (a) before and (b) after the introduction of disilane.

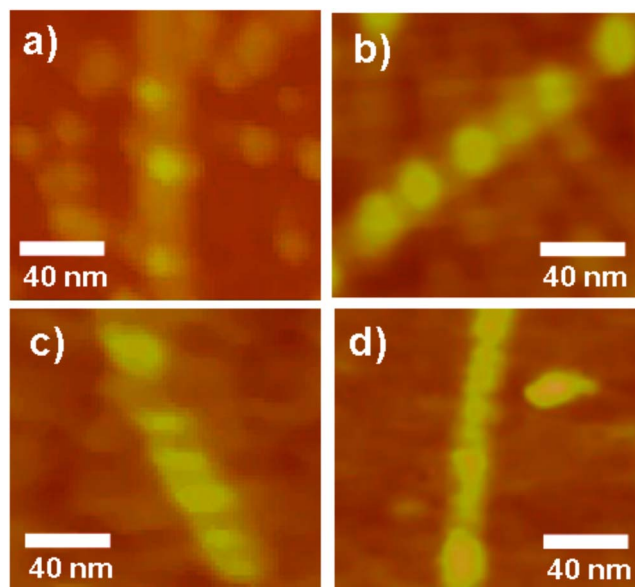


FIG. 3. (Color online) AFM image of four samples that were grown at different Si₂H₆ flow rate: (a) 1.1 SCCM, (b) 1.6 SCCM, (c) 1.8 SCCM, and (d) 2.1 SCCM.

QDs. This is due to the fact that with a higher flow rate there is more source material depositing over the substrate at any given time. More source impingement increases the opportunities for a Si atom to find a high strain point and settle to form a seed, which in turn will form a QD. This behavior has also been observed in QDs grown on HfO₂ patterned surfaces.¹⁰ In contrast, if less Si is deposited then the chances for strain driven alignment are fewer and more QDs start to form over the rest of the substrate, as can be seen in Fig. 3(a). The size of each image is 200 × 200 nm². Due to tip deterioration some of the QDs appear larger in base than the others. Base size is dependent strictly on the size of the ridge created by the CNT since the formation of a valley at the edges of the CNT is expected to have a greater surface energy. This pattern of size limitation can be seen throughout the different flow rates in the QD growth. Figure 4(a) plots the linear density of QDs as a function of the gas flow rate.

Figure 4(b) shows the linear density of the QDs on CNT as a function of growth time. Coincidentally the effects of time

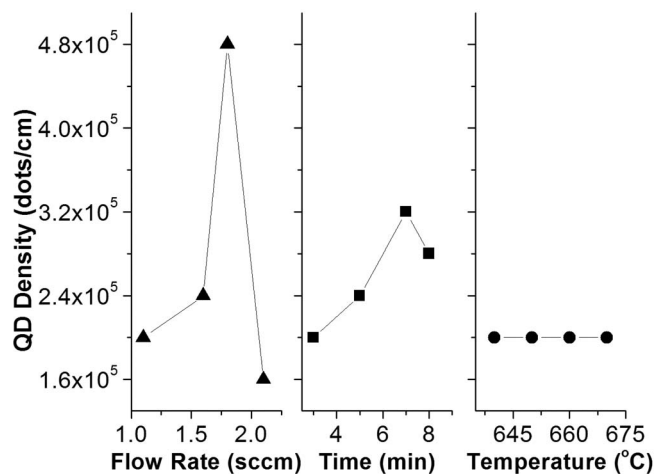


FIG. 4. Linear density of QDs on CNTs as a function of (a) flow rate, (b) growth time, and (c) growth temperature.

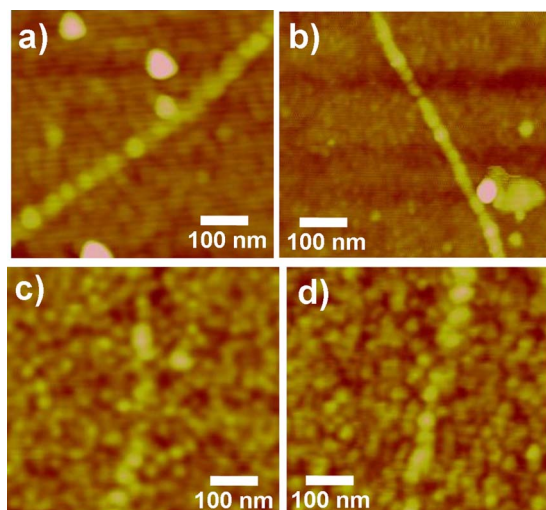


FIG. 5. (Color online) AFM images of four samples that have different hafnium oxide thickness: (a) 6 nm, (b) 7 nm, (c) 7.6 nm, and (d) 8 nm.

on the linear density resulted similar to the trend observed with varying the flow rate. The linear density increases with increasing time at the initial stage. For longer growth time, the QD density starts to decrease. The trend of the increase of linear density continues until the QDs exceed a certain size close to the width of the CNT ridge. The edge of the ridge is the threshold for the QD growth along the CNT. As the QD size reaches that threshold, the strain created by the CNT is compensated and growth past the edges of the 1D ridges is accelerated.

Figure 4(c) shows the growth temperature effect on the linear density of the dots on CNT. Interestingly different temperatures have a negligible effect on QD density in the window of alignment. Since growth temperature is known to affect adatom diffusion length,^{15,16} it is reasonable for Si adatoms that are farther from CNT ridges in the initial stages of growth to migrate over to the alignment sites at higher growth temperature. In the examined temperature range, sufficient number of Si adatoms can migrate to preferential nucleation sites on 1D HfO₂ ridges on CNTs. Until the strain distribution along the 1D ridge becomes periodic, this is responsible for periodic aligned QDs. Such “cooperative” regimented growth mode was also observed when Ge dots were grown on 1D Si ridges.⁸ This correlates with our low temperature results (not shown here) that show no alignment due to a low diffusion length. Another reason for a constant density with respect to temperature is that surface desorption of Si adatoms also increases with respect to temperature.¹⁰

To study different strain conditions created by the underlying CNT, we varied the oxide thickness. The effects created by the increase in oxide thickness can be seen in Figs. 5(a)–5(d). The thicker the oxide is, the sharper QDs are around the CNT ridge. This is due to the relaxation of the strain that forms along the top of the ridge structure. This in

turn will decrease the selectivity of Si adatoms, forming more QDs on flat areas of the substrate. Although atomic layer deposition is conformal to most surfaces, CNTs are known to be nonreactive to the H₂O precursor.¹³ Therefore many more HfO₂ layers are needed to be deposited to fully cover the CNT and have a smooth surface for good Si migration. The window of selectivity starts close to the 6 nm mark and decreases after 1–2 nm depending on the size of the ridge, which is dependent on the diameter of the CNT.

In summary, we have successfully aligned Si QDs on strained HfO₂ covered CNTs. We studied the effects of growth temperature, disilane flow rate, and oxide thickness on the density of the QDs on the 1D HfO₂ ridges created by the underlying CNTs. We found that the size of the ridge created by the CNT dictates the maximum size of the QDs but the effect is diminished with the increase of the oxide thickness. In addition, the changes in disilane flow rate and growth time showed that the density of the QDs on the ridges can be controlled as well as the QD deposition outside of the ridges. These results show that the alignment of QDs by a bottom up approach to a size beyond CMOS ultimate limit is possible and controllable.

The authors acknowledge the financial and program support of the Focus Center Research Program (FCRP) on FENA and the National Science Foundation (NSF) (Contract No. DMR 0807232). C.N.L. and G.L. acknowledge support by NSF CAREER Grant No. DMR/0748910 and ONR/DMEA Grant No. H94003-07-2-0703.

¹D. W. Kim, T. Kim, and S. K. Banerjee, *IEEE Trans. Electron Devices* **50**, 1823 (2003).

²J. J. Lee, X. Wang, W. Bai, N. Lu, and D. L. Kwong, *IEEE Trans. Electron Devices* **50**, 2067 (2003).

³N. M. Park, T. S. Kim, and S. J. Park, *Appl. Phys. Lett.* **78**, 2575 (2001).

⁴Z. T. Kang, B. Arnold, C. J. Summers, and B. K. Wagner, *Nanotechnology* **17**, 4477 (2006).

⁵F. Eroghogbo, K. T. Yong, I. Roy, G. Xu, P. N. Prasad, and M. T. Swihart, *ACS Nano* **2**, 873 (2008).

⁶S. J. Angus, A. J. Ferguson, A. S. Dzurak, and R. G. Clark, *Nano Lett.* **7**, 2051 (2007).

⁷C. Taylor, E. Marega, E. A. Stach, G. Salamo, L. Hussey, M. Muñoz, and A. Malshe, *Nanotechnology* **19**, 015301 (2008).

⁸G. Jin, J. L. Liu, S. G. Thomas, Y. H. Luo, K. L. Wang, and B. Y. Nguyen, *Appl. Phys. Lett.* **75**, 2752 (1999).

⁹G. Jin, J. L. Liu, and K. L. Wang, *Appl. Phys. Lett.* **76**, 3591 (2000).

¹⁰S. S. Coffee and J. G. Ekerdt, *J. Appl. Phys.* **102**, 114912 (2007).

¹¹S. Han, X. Liu, and C. Zhou, *J. Am. Chem. Soc.* **127**, 5294 (2005).

¹²P. Jarillo-Herrero, J. A. Van Dam, and L. P. Kouwenhoven, *Nature (London)* **439**, 953 (2006).

¹³A. Javey, J. Guo, D. B. Farmer, Q. Wang, E. Yenilmez, R. G. Gordon, M. Lundstrom, and H. Dai, *Nano Lett.* **4**, 1319 (2004).

¹⁴S. J. Tans, M. H. Devoret, H. Dai, A. Thess, R. E. Smalley, L. J. Geerligs, and C. Dekker, *Nature (London)* **386**, 474 (1997).

¹⁵J. Tersoff, C. Teichert, and M. G. Lagally, *Phys. Rev. Lett.* **76**, 1675 (1996).

¹⁶Q. Xie, A. Madhukar, P. Chen, and N. P. Kobayashi, *Phys. Rev. Lett.* **75**, 2542 (1995).